A Forward Impulse Radiating Antenna for Subsurface Radars

A. Teggatz, A. Jöstingmeier, T. Meyer, and A. S. Omar

Institute of Electronics, Signal Processing and Communications, FEIT, University of Magdeburg
P.O. Box 4120, Universitätsplatz 2, 39106 Magdeburg, Germany, ateggatz@iesk.et.uni-magdeburg.de

***Abstract* — We will present a novel forward impulse radiating antenna (IRA) that has been optimized for subsurface radar applications using a 3d field simulator. Though this antenna possesses an inferior return loss compared to antennas developed for free space applications it yields images of subsurface objects with outstanding resolution when an appropriate calibration technique is applied. This technique locates the reference plane inside the ground and allows for removing the air-ground reflection as well as the antenna mismatch and losses. A prototype of the new antenna has already been built and will be presented.**

I. Introduction

The detection of buried objects such as landmines or unexploded ordnance by means of ground penetrating radar (GPR) is an intensely investigated field of research. The antenna is the crucial hardware part of a GPR system because the imaging quality is strongly depending on the radiation characteristics of the antenna. The antenna parameters that have to be optimized according to the applied data processing algorithms include bandwidth, radiation pattern, phase center location, gain and radiation efficiency. Usually antennas are designed for free space applications. However, in a GPR the antenna has to meet completely different requirements since it is often located very close to the ground in order to receive a strong target signal. Therefore GPR antennas cannot be optimized without taking the environment into account.

In [1] it has already been demonstrated how the electromagnetic field simulator Microwave Studio (MWS) can be used to optimize the design of GPR antennas. The quality of an antenna is assessed by a series of B-scans for typical targets. Since a single B-scan already requires a large number of simulation runs it is necessary to automate the process of the antenna movement above the ground. This task is accomplished by controlling the field simulation tool from the main GPR simulation application by means of ActiveX.

The GPR simulator has been used to investigate a variety of antennas such as standard gain horns, TEM horns, conical spirals, log-periodic antennas and other types some of which have already been investigated in [2]. All of these antennas suffer from the disadvantage that the reflection at the air-soil interface is much stronger than the target reflection itself. Therefore we have suggested a novel forward radiating IRA which is named Orion-type due to its shape that resembles the Orion star ship. Simulations show that this antenna gives superior results concerning the detection of buried objects when it is used together with the calibration technique that will also be presented within this contribution. Figs. 1 and 2 show the MWS model of the proposed Orion-type IRA.

II. Orion Antenna

The Orion-type antenna is mainly a forward radiating IRA with two metal arms, embedded in a dielectric material. The permittivity of this dielectric cone has been chosen close to the permittivity of the soil. Thus the overall mismatch due to the soil-air and the air-antenna interface can be decreased as the antenna is installed very close to the ground surface. In the investigated setup the distance between the IRA and the ground is only 10 mm. The cone is made of AK4 low loss dielectric material [3]. The relative permittivity of this material is almost frequency independent 3.85 which has been determined by a precision broadband measuring method [4].

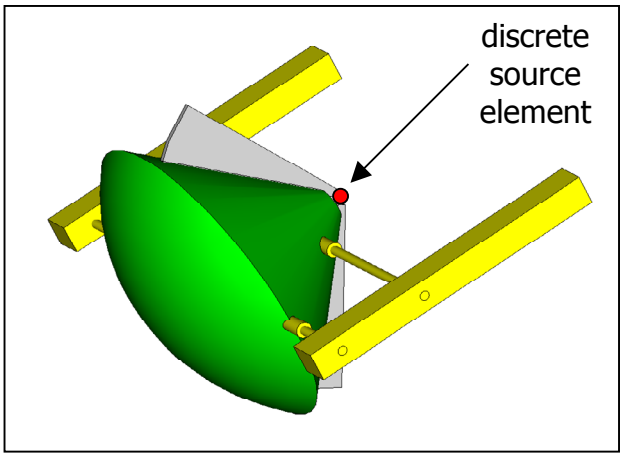

Fig. 1. Microwave Studio model of the Orion-type IRA.

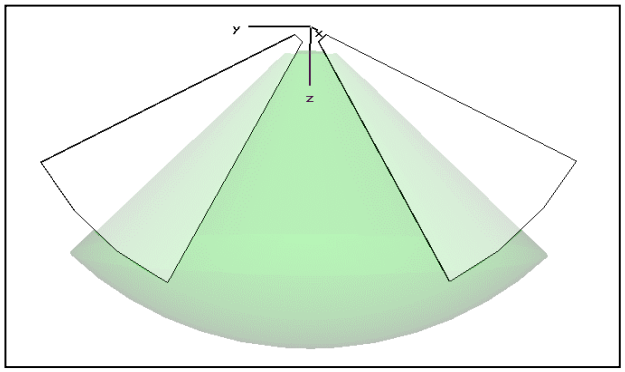

Fig. 2. Position of the metal arms inside the dielectric cone.

For feeding the antenna it is necessary to use a balun with a step up ratio of 4:1 in order to match the 50 Ohm feeding line impedance to the radiation impedance of the antenna that is about 200 Ohm. Furthermore the balun connects the unsymmetrical coaxial line with the symmetrical antenna structure and eliminates its common mode excitation. The free space performance of the Orion-type IRA strongly depends on the operating frequency. Fig. 4 indicates a poor directivity of the antenna at 1 GHz while Fig. 5 shows a pencil beam like radiation pattern that has been observed at 5 GHz. Moreover the return loss of the Orion-type IRA which is presented in Fig. 6 is quite large compared to that of other antennas which have been optimized for free space operation. For example in Fig. 7 the measured and the simulated return loss of a double ridged TEM horn are given. Such horns have also been used in subsurface detection applications. Comparing the results presented in Figs. 6 and 7, it is obvious that the free space performance of the Orion-type impulse radiating antenna is inferior to that of the TEM horn.

However, it has been found from the simulations of the entire GPR environment that the Orion-type IRA basically illuminates the small area directly below the cone, and that the wave propagation in this region is in a good agreement to that of a wave traveling along a 1d transmission line. This is important because in order to apply a one-port calibration technique a 1d transmission line model must be valid for the field propagating inside the ground. Figs. 8 and 9 show the simulated radiation of the Orion-type IRA at 2 GHz in the presence of homogeneous soil with a permittivity of ε_r=3. On the other hand, the TEM horn has an aperture which is much larger then the transverse dimensions of the Orion-type IRA leading to a wave propagation inside the ground which cannot be described by a 1d transmission model.

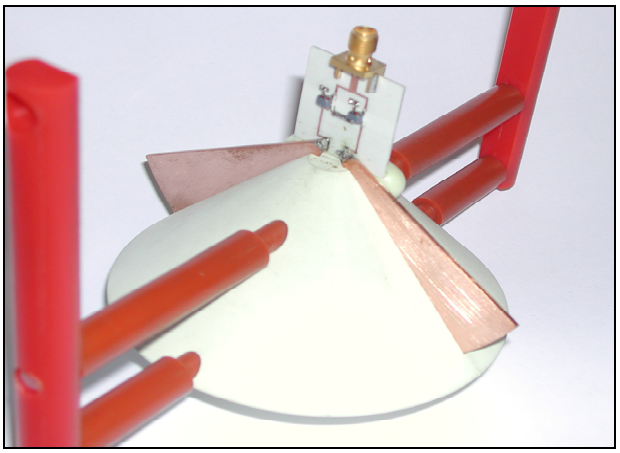

Fig. 3. Prototype of the Orion-type antenna.

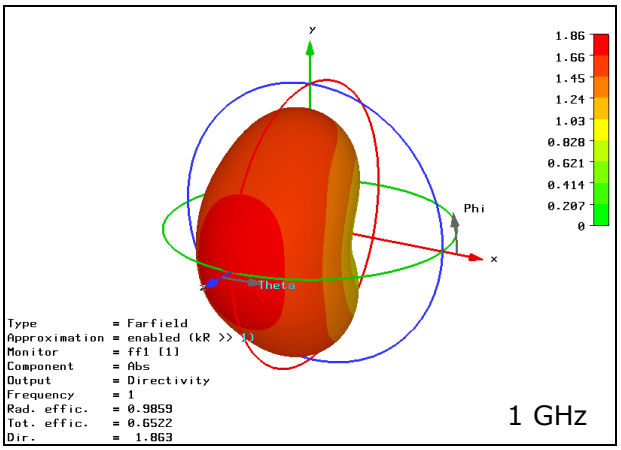

Fig. 4. Radiation pattern of the IRA at 1 GHz.

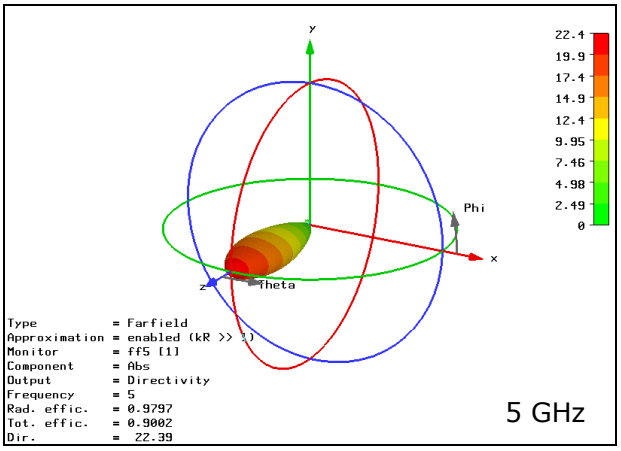

Fig. 5. Radiation pattern of the IRA at 5 GHz.

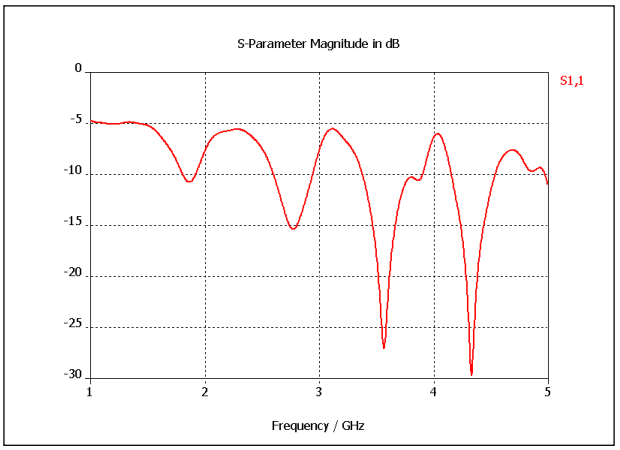

Fig. 6. Return loss of the Orion-type IRA for 1 GHz-5 GHz.

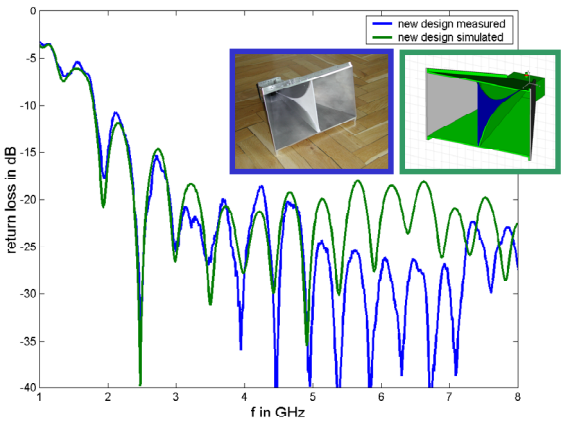

Fig. 7. Return loss of a TEM horn for 1 GHz-8 GHz.

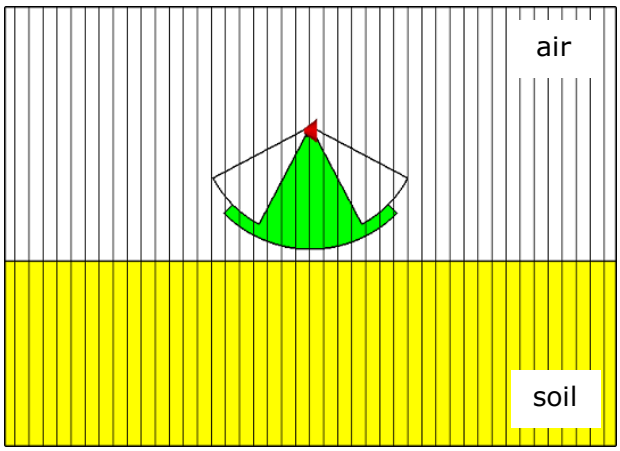

Fig. 8. MWS setup for the simulation of the radiation.

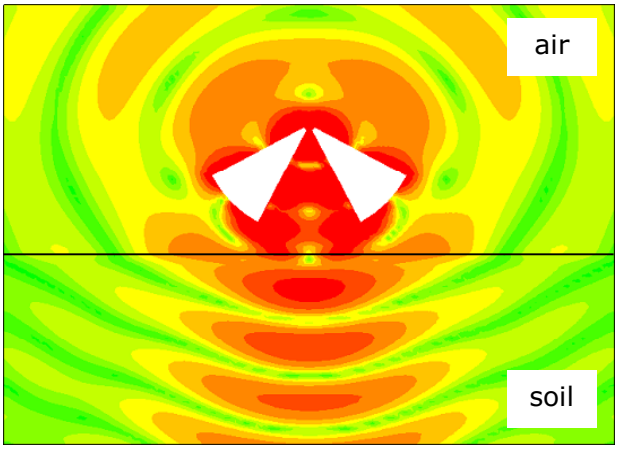

Fig. 9. Simulated radiation in the presence of soil at 2 GHz.

III. Calibration Procedure

A. Calibration Standards

Following the well-known standard one-port calibration procedure one has to take three different calibration standards into account, which are usually a match, a short and an offset short. Adapting this procedure to subsurface detection match means that the antenna radiates above the homogeneous ground for which we assume the relative permittivity of dry sand, namely, ε_r=3.

The second standard, which is the short, defines the position of the reference plane. This standard is just a large metal plate located inside the ground at the depth of the reference plane. Since we are interested in the detection of targets that are buried within the first 200 mm underneath the surface, we put the reference plane at the center of this region, located at a depth of 100 mm. Finally we have to apply one or more offset shorts. The number of these offset short standards depends on the considered frequency range for the measurement. In our case the GPR utilizes the frequency range from 1 GHz to 5 GHz which is supposed to be a common frequency range for GPR. Accordingly, two offset shorts with offsets of 22 mm and 8 mm, respectively, have been chosen. This guarantees that the additional line length which is introduced by the two offsets leads to a phase shift within an interval of 90° ± 25° at any frequency in the considered range. Hence the equations for the error terms are sufficiently independent.

B. Error Coefficients

The time domain signals reveal that the antenna mismatch and the air-surface reflection have even a stronger effect than the reflections corresponding to the short and the offset short standards. The parameters of the error model [5] E_R, E_D and E_S are calculated from the corresponding frequency domain data. These error coefficients are a function of the frequency. Fig. 10 shows that they are continuous as expected at the transition frequency at which the calibration procedure switches from the first offset short to the second one.

$$S_{corr} = \frac{S_{meas} - E_D}{E_R + E_S (S_{meas} - E_D)} \qquad (1)$$

The measured reflection coefficient is corrected by applying equation (1). The measured and the corrected reflection coefficient are denoted by S_{meas} and S_{corr}, respectively. Keeping in mind that E_D is just the measured reflection when the match standard is applied, the calibration procedure can be substituted by a simple so called background subtraction. In this case the term $E_S (S_{meas}-E_D)$ is considered to be small compared to the value of E_R. However the exclusive application of a background subtraction does neither yield the exact depth nor the accurate reflectivity of the buried object.

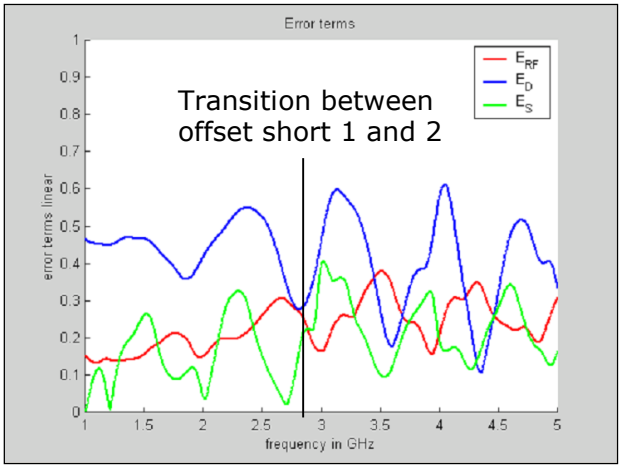

Fig. 10. Transition between the error coefficients.

IV. Experimental Results

Fig. 12 shows what happens when the above-discussed correction is applied to an air layer located exactly at the position of the reference plane, that has been placed 100 mm underneath the surface of the ground. The antenna mismatch and the surface reflection, that appear in the Fig. 13, are completely eliminated after the application of the calibration procedure.

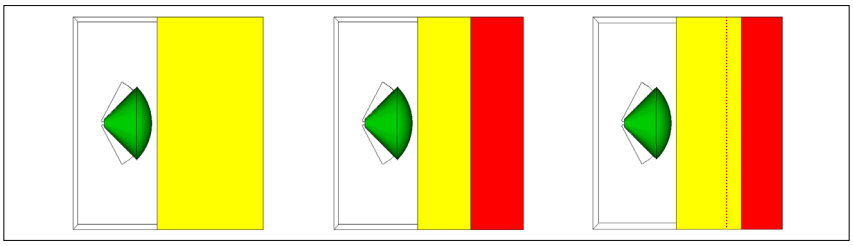

Fig. 11. Calibration standards - match, short and several different offset short.

At the same time the target signal, that appears to be weaker than the other reflections in the data without calibration, is obtained according to (2).

$$\Gamma = \left(\sqrt{\varepsilon_{rB}} - \sqrt{\varepsilon_{rO}}\right) / \left(\sqrt{\varepsilon_{rB}} + \sqrt{\varepsilon_{rO}}\right) \qquad (2)$$

The value of the corrected reflection coefficient is exactly the theoretical value given by (2), where ε_{rB} and ε_{r0} are the permittivity of the background and the permittivity of the object, respectively. Furthermore the depth of the target is well-defined with respect to the reference plane in a depth of 100 mm. The performance of an ordinary background subtraction (results in Fig. 14) is inferior compared to the calibration procedure.

V. Conclusion

A novel forward radiating IRA concept has been introduced. The proposed antenna is suitable for subsurface radar applications. A GPR system using this antenna can be calibrated with respect to a reference plane inside the ground. The ability of the method to increase the accuracy and the performance of the GPR detection of buried objects has been demonstrated. The antenna mismatch and the air-surface reflection can be removed from the original data if the discussed error model will be applied. Hence the antenna gives superior results concerning the achievable resolution when it is used together with the suggested calibration technique.

References

[1] A. Teggatz, A. Jöstingmeier, T. Meyer and A. S. Omar, Simulation of a Ground Penetrating Radar Environment by Means of FDTD Methods Using an Automatic Control Approach, IEEE AP-S / URSI Int. Symp. Digest, vol. 2, pp. 2095-2098, Monterey, USA, June 2004.

[2] R. V. de Jongh, A. G. Yarovoy, L. P. Ligthart, I. V. Kaploun A. D. Schukin, Design and Analysis of new GPR antenna concepts, in Proc. 7th Int. Conference On Ground-Penetrating Radar (GPR´98), vol. 1, pp. 81-89, Kansas, USA, May 1998

[3] Cuming microwave corporation, C-Stock AK4 Datasheet http://www.cumingmw.com/micro_dielectric.html.

[4] A. Jöstingmeier, T. Meyer and A. S. Omar, Material Measurements of Absorbers with Magnetic Losses, IEEE AP-S / URSI Int. Symp. Digest, vol. 4, pp. 66, Columbus, USA, June 2003.

[5] M. Thumm, W. Wiesbeck und S. Kern, Hochfrequenz-messtechnik, BG Teubner, Stuttgart, Germany, 1998.

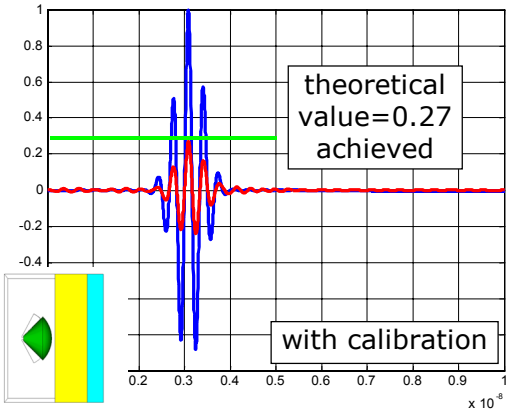

Fig. 12. Air layer object in the ground with calibration.

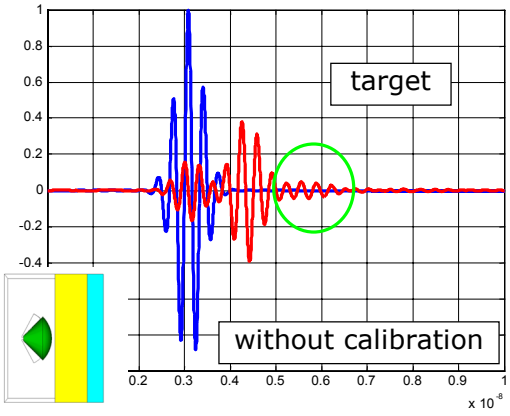

Fig. 13. Air layer object in the ground without calibration.

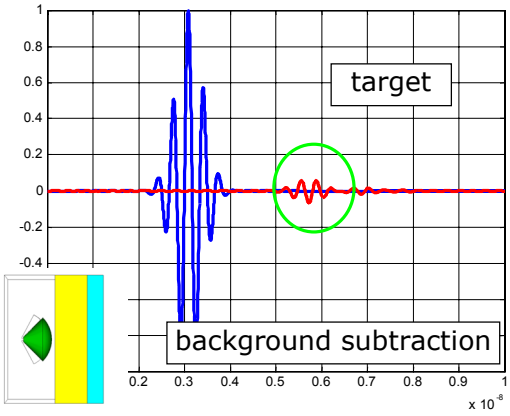

Fig. 14. Air layer object with background subtraction only.